Iraqi J. Laser, issue 1, vol., 22, pp. 43-50 (2023)

IRAQI JOURNAL OF LASER

The effect of nanoelectrodes number and length on enhancing the THz photomixer performance

*Reiam Al-Mudhafar, Hussein Ali Jawad**
Corresponding author: Hussein@ilps.uobaghdad.edu.iq
Institute of Laser for Postgraduate Studies, University of Baghdad, Baghdad, Iraq

(Received 23/01/2023; accepted 30/03/2023)

Abstract: Despite the distinct features of the continuous wave (CW) Terahertz (THz) emitter using photomixing technique, it suffers from the relatively low radiation output power. Therefore, one of effective ways to improve the photomixer emitter performance was using nanodimensions electrodes inside the optical active region of the device. Due to the nanodimension sizes and good electrical conductivity of silver nanowires (Ag-NWs), they have been exploited as THz emitter electrodes. The excited surface plasmon polariton waves (SPPs) on the surface of nanowire enhances the incident excitation signal. Therefore, the photomixer based Ag-NW compared to conventional one significantly exhibits higher THz output signal. In this work, the effect of Ag-NWs dimensions and number on the incident optical field is investigated by utilizing the Computer Simulation Technology (CST) Studio Suite. The simulation results show that increasing Ag-NWs length to SPP propagation length ratio plays a significant role on the incident field increment due to its effect on reducing the SPP propagation losses. The increment of Ag-NWs number and length in the nanoelectrodes based photomixer can contribute to increase the electric field in the active region by 1.5 times at the longer excitation wavelength (850 nm). As a result of this increment, the THz output power and the conversion efficiency are expected to be enhanced by a factor of five.
Keywords: Plasmonics, Silver nanowire, Terahertz photomixer

1. Introduction

The CW-THz emitters using photomixing technique offer many distinctive features in terms of compactness, cost, tunability, and wavelength resolution [1 - 3]. A photomixing technique is based on optical beat signal of two CW laser beams of slightly difference frequencies (which must be in THz frequency region). This signal, which oscillates at the two lasers difference frequency, is used to excite a photoconductive material and then modulates the photocarriers generation [4, 5]. The photocarriers are collected by electrodes and then translated into THz radiation by an antenna connected to the device [6, 7]. However, the conventional photomixer suffers from its low optical to THz conversion efficiency [6, 8]. Several research works have been attempted to improving the THz output power by enhancing the incident optical intensity inside the photomixer [9 - 13]. The high optical intensity improves the gained photocurrent and thus increases the output radiation. In CW-THz photomixer, Ag-NWs are used as nanodimension electrodes to drive and collect the excited carriers of photoconductive material [14, 15]. Due to small size of these

nanowires, the photomixer devices based on Ag-NWs gain remarkable features [14]. The nanodimensions of these metallic wires give rise to reduce the device capacitance. Furthermore, the electric field of surface SPPs excited on the interface between the Ag-NW and the photoconductive material undergoes notable enhancement. Both factors contribute to improve the photogenerated current inside the mixer active area. Therefore, the photomixer based Ag-NW compared to conventional one significantly exhibits higher obtained photocurrent [15].

In this work, the electric field of SPPs on the surface of Ag-NWs placed on photomixer conductive material (GaAs) is investigated. Therefore, the active region comprises the nanoelectrodes and photoconductive material is simulated by utilizing the CST Studio Suite. From the simulation work, the effect of Ag-NWs dimensions and number on the electric field inside the photomixer can be examined and scrutinized.

2. Theory

The photomixer output power P_{THz} in terms of optical incident intensity is expressed as [16]:

$$P_{THz}(\omega_{THz}) = \frac{1}{2} R_A . (E_{DC}^2 I_o^2) . \frac{\tau_c^2 \mu_e^2}{1+ \omega_{THz}{}^2 \tau_c^2} \quad (1)$$

where R_A is the antenna radiation resistance, E_{DC} is the bias field, I_o is the beat optical intensity, τ_c is carriers lifetime, μ_e is carriers mobility, $\omega_{THz} = \omega_1 - \omega_2$ is the THz frequency of beat signal, and ω_1, ω_2 are the frequencies of two incident lasers.

The optical to THz conversion efficiency of the photomixer is[17]

$$\eta = \frac{P_{THz}(\omega_{THz})}{P_1 P_2} \quad (2)$$

where P_1, and P_2 the optical powers of two incident lasers.

In Ag-NW based photomixer, SPP waves are excited on the surface of the metallic wire by laser light polarized along the wire axis [17, 18]. The incident light is scattered from the wire surface generating SPP modes which propagate towards the end of the wire [17, 19]. The propagating SPPs waves generally reflect at the end face of nanowire of finite length. The reflection of surface plasmon at the end face leads to produce modulation of SPPs field on the surface of nanowire. The spectral modulation depth $\Delta I/I_{min}$ on Ag-NW surface can be determined from [20, 21]:

$$\frac{\Delta I}{I_{min}} = \frac{4RA}{(1-RA)^2} \quad (3)$$

where R is the Ag-NW end face reflectivity, A is the propagation loss which is given by [23]

$$A = e^{-L_{NW}/L_{SPP}} \quad (4)$$

where, L_{NW} is the length of nanowire, L_{SPP} is the SPP propagation distance is given by [23, 24]:

$$L_{SPP} = \frac{\lambda}{2\pi} \left(\frac{\varepsilon_d+\varepsilon_{mr}}{\varepsilon_d \varepsilon_{mr}}\right)^{3/2} \left(\frac{\varepsilon_{mr}^2}{\varepsilon_{mi}}\right) \quad (5)$$

where, λ is optical wavelength of incident light, ε_d is the dielectric constant of dielectric material and ε_{mr}, ε_{mi} are the real and imaginary parts of the metal dielectric constant, respectively.

3. Experiment and Results

By using electromagnetic (EM) software program, we evaluated the near field enhancement in the photomixer after exciting SPPs of Ag-NWs. Simulating the entire nanodimension photomixer (the active region and connected antenna) will take up a great deal of calculation time. For this reason, only the active region is simulated rather than simulating the whole device. Consequently, the active region comprises the nanoelectrodes and photoconductive material is simulated by utilizing CST. The electric field distribution is calculated in the photomixer active region for each value of Ag-NWs number and length. Thereafter, we can scrutinize the electric field in each case and investigate the effect of the Ag-NWs structure parameters on the field variation.

The simulation method is described and clarified in two separate parts. The first part presents the descriptions of the structure parameters, dimensions, materials that used in the simulation. The simulation procedure and methods are then explained in the second part.

Active region of Ag-NWs based photomixer: Firstly, the Ag-NWs number in the active region is varied with three values (2, 6, and 10 nanowires). Fig. (1) illustrates three active region structures of Ag-NWs based photomixer of different electrodes numbers. Secondly, L_{NW} is also changed with four values (3, 3.5, 4, and 4.5 μm). The structures consist of Ag-NWs nanoelectrodes placed on a photoconductive material (the device substrate). Each structure has the area of 10 x 10 μm^2. The

length of the used nanowires is 4.5 μm, and the gap between their end faces is 1 μm. GaAs (12.94 relative permittivity) is used as a substrate. The thicknesses of the electrodes and substrate material are 0.120 μm and 1 μm, respectively. The structures of 6 and 10 Ag-NWs have 2.5, 1.5 μm electrodes space, respectively, to obtain an even distribution of nanowires on the substrate surface.

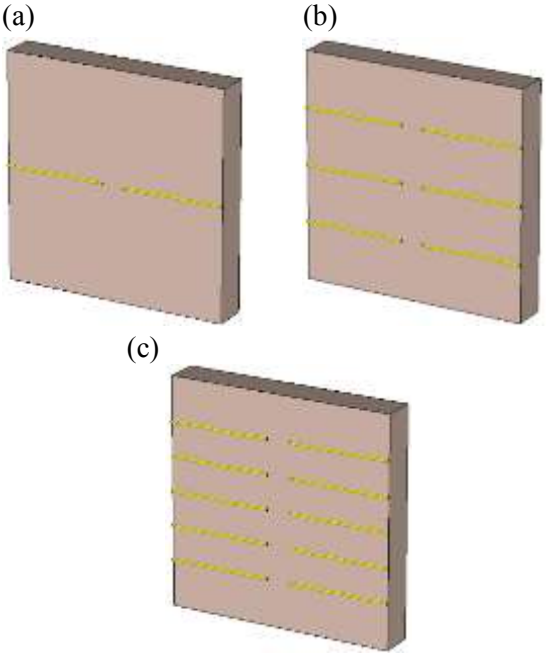

Fig.1: Schematic diagram of THz photomixer active regions of different Ag-NWs number: 2, 6, and 10 presented in (a), (b), (c), respectively. The active region of 6 and 10 Ag-NWs have 2.5, 1.5 μm electrodes space, respectively, to obtain an even distribution of nanowires on the substrate surface.

Simulation of the active region of Ag-NWs based photomixer: The active region of the photomixer is simulated using CST program to calculate the electric field distribution after illuminating with optical signal. The EM simulation of the electric field distribution on the structure surface is carried out using time domain solver (TDS).

To generate CW-THz radiation, the photomixer active material must be excited by CW optical signal. This optical signal takes a form of beat signal of two optical beams (from two CW semiconductor lasers) which are slightly different in THz frequency range ($\omega_{THz} = \omega_1 - \omega_2$). Since, their frequencies are in optical region and the difference between them is in THz frequency, therefore; their photon energies are close to each other and the photoconductive material interact with them as an optical beam of single frequency. In the simulation, this beat signal was represented as a plane wave of linear polarization. It is incident on the structure side that contains the nanoelectrodes. The electric field of incident plane wave is 1 V/m. The band gap energy of GaAs is 1.42 eV. Therefore, the laser signal with optical signal near or higher than (1.42 eV) can be used to excite GaAs. The excitation wavelength of conventional photomixer lies in near infrared (NIR) region of EM spectrum (to obtain an optical signal can beat in THz frequency). Therefore, the incident wavelengths 780, 810, and 850 nm are commonly chosen to excite the photomixer.

Because of the inability to work with optical and THz frequency ranges in a single simulation and in order to reduce the large computational time of simulating the nanodimension structures, only the active region is simulated rather than the whole device. 6-mesh-cells per incident wavelength are considered in the structure simulation. On the other hand, a local mesh of 3-cells is set for precisely simulating the electrodes nanodiameter.

In this work, the effect of Ag-NWs electrodes number and length on the optical near field is investigated in the photomixer. At the beginning, the number of Ag-NWs is changed and the consequent variation of the optical electric field in the active region is calculated. In the simulation, the adopted Ag-NWs numbers are: 2, 6, and 10. Thereafter, the Ag-NWs number is fixed and their length is changed with four values: 3, 3.5, 4, and 4.5 μm. Subsequently, the change in the optical electric field is scrutinized for each case.

The simulation results were obtained after illuminating the active region with linearly polarized plane wave of NIR frequency. From the results, we scrutinize the influence of Ag-NWs number and length on the maximum optical near field. At first, the active region structures of three different numbers of Ag-NWs were simulated. The EM simulation using time domain solver is carried out to calculate the resultant electric field on the surface of active region. After the optical illumination, the SPPs wave will be excited on the Ag-NWs surface. The maximum electric field as function of Ag-NWs number for the three incident wavelengths is illustrated in Fig (2). As it can be seen from the figure, the field is significantly enhanced for 780 and 850 nm incident wavelengths when the

nanowires are added to the structure. The electric field is enhanced by the factor of two when the Ag-NW number is changed from 0 to 2 nanowires. The reason behind this enhancement is the plasmonic field induced by Ag-NW. Ag-NW will enhance the field over the whole GaAs surface, therefore; this field is increased with increasing the nanowire number on this surface. A larger number of Ag-NW means more reinforcement to the nanowire plasmonic field on the semiconductor surface.

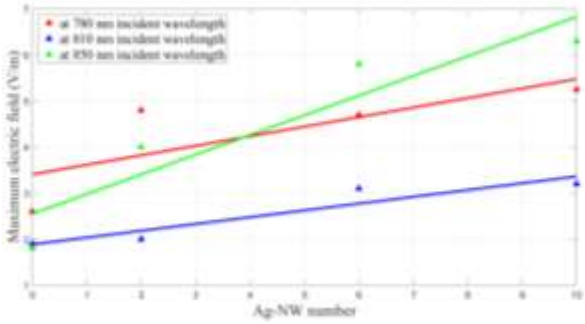

Fig.2: Maximum electric field (colored triangles) calculated in the photomixer active region as a function of Ag-NWs numbers. The colored lines represent the results fitted curves.

It can be noticed from Fig. (2) that the plasmonic effect of Ag-NW is small at 810 nm wavelength, since the electric field is not clearly changed after adding Ag-NW. However, this field is significantly increased by a factor of two when the Ag-NW number is changed from 2 to 10. This means that the plasmonic field is small at 810 nm but it exhibits notable increment when the nanowires number is raised due to boosting the light confinement by the Ag-NWs small dimensions. From the results, the maximum electric field is directly proportional to the nanowires number. For larger Ag-NWs numbers, the maximum electric field is noticeable increased on the surface of the active region. The highest increment in the electric field is at 850 nm.

The distribution of the electric field, at 850 nm incident wavelength, in the active regions of different Ag-NWs numbers: 0, 2, 6, 10 are shown in Fig. (3). It can be seen from Fig. (3) that field localizations can be noticed in all structures of Ag-NWs electrodes. It substantially occurs at the two face ends of Ag-NWs. The reason of this noticeable localization is the reflecting of SPPs waves at the end edge of Ag-NW [21].

Figure (4) shows the simulation results of current density in the photomixer active region for different Ag-NWs numbers. The results show that the current density is also directly proportional to the nanowire number. Increasing the electric field with Ag-NW number means higher light intensity can be obtained (more carriers can be generated on the GaAs surface). The large carrier number contributes to enlarge the nanowire conductivity in the active region of photomixer. Therefore, one can see higher value of Ag-NW current density with increasing nanowire number. Due to the small value of the electric field at 810 nm incident wavelength, the current density in the active region is small as compared to that of the other two wavelengths.

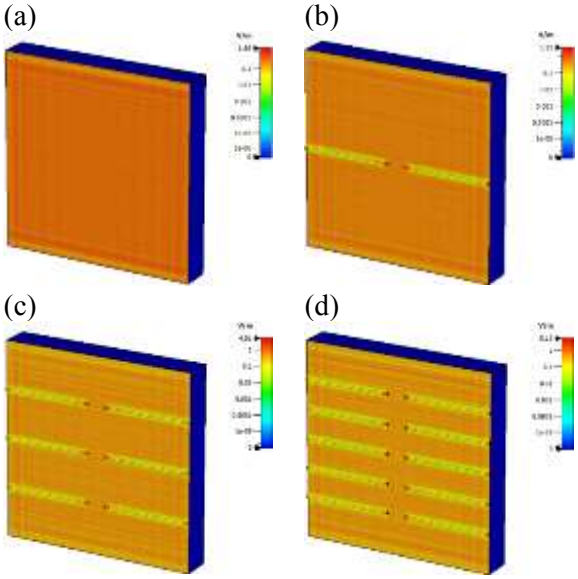

Fig.3: Distribution electric field, at 850 nm incident wavelength, in the active regions of different Ag-NWs numbers: 0, 2, 6, 10 presented in (a), (b), (c), and (d), respectively.

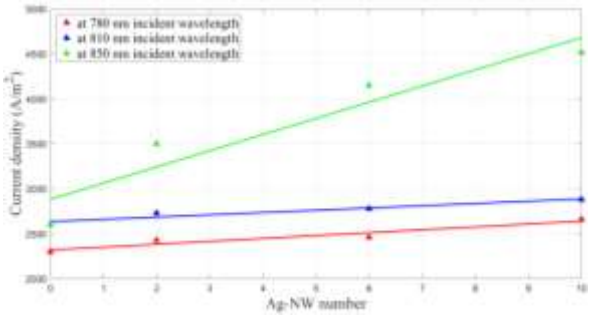

Fig.4: Current density (colored triangles) calculated in the photomixer active region as a function of Ag-NWs numbers. The colored lines represent the results fitted curves.

The effect of L_{NW} on the near electric field is additionally investigated in the photomixer active region. Four active region structures of different Ag-NW lengths (L_{NW} = 3, 3.5, 4, and 4.5 μm) were simulated. The active regions have dimensions of 10 ×10 μm^2 and the Ag-NWs is fixed at the number which shows the highest obtained field (10 Ag-NWs). The maximum electric field in the photomixer active region as a function of L_{NW} is illustrated in Fig. (5). The electric field is increased with L_{NW}. At 850 nm, the electric field is increased from 4.25 V/m to 6.3 V/m when L_{NW} is changed from 3 μm to 4.5 μm. The electric field is significantly changed at 810 and 850 nm incident wavelengths. On the other hand, it is less affected by L_{NW} at 780 nm wavelength. Consequently, the electric field dependency on L_{NW} is directly proportional to the excitation wavelength, i.e. it is comparatively high at longer wavelength (lower excitation frequency).

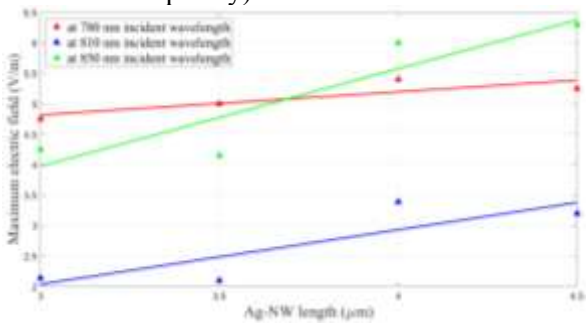

Fig.5: Maximum electric field (colored triangles) calculated in the photomixer active region as a function of Ag-NWs lengths. The colored lines represent the results fitted curves.

The electric field distributions in the active regions of four L_{NW} lengths (3, 3.5, 4, 4.5 μm) are illustrated in Fig. (6). The calculated current density in the photomixer active region as a function of Ag-NWs number is illustrated in Fig. (7). The current density does not show any change in the its values at 780, and 810 nm wavelengths. The small change in electric field with L_{NW} at 780 nm wavelength causes the relatively stable value of current density at this wavelength. As the electric field is less affected by the Ag-NWs at 810 nm wavelength, the change in current density in the active region is very small at this wavelength.

The propagation losses, which determine the spectral modulation depth $\Delta I/I_{min}$ on Ag-NW surface, would have a low value at long L_{NW} according to Eq. (4). For this reason, the electric field in the active region shows an increment in its value with L_{NW}, as shown in Fig. (5). The propagation losses of SPP are calculated by using Eq. (4) for each value of L_{NW}. Before calculating the propagation losses, we need to determine L_{SPP} on the Ag-NW interface with GaAs. Eq. (5) is used to calculate L_{SPP} for all excitation wavelengths. Table (1) shows the calculation results of L_{SPP} for each wavelength.

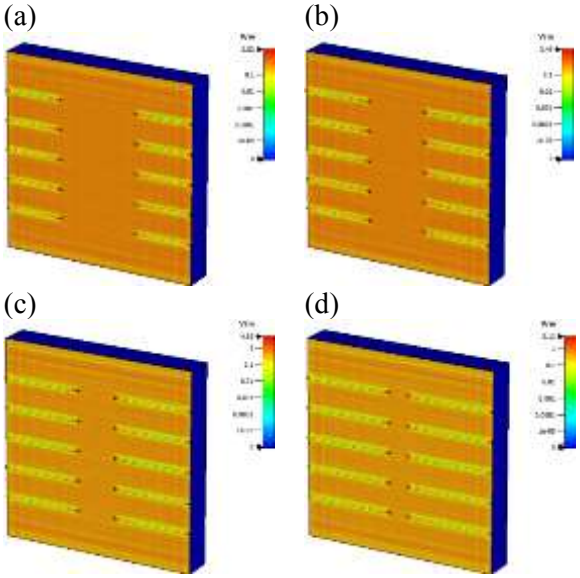

Fig.6: Distribution electric field, at 850 nm incident wavelength, in the active regions of different Ag-NWs lengths: 3, 3.5, 4, and 4.5 presented in (a), (b), (c), and (d), respectively.

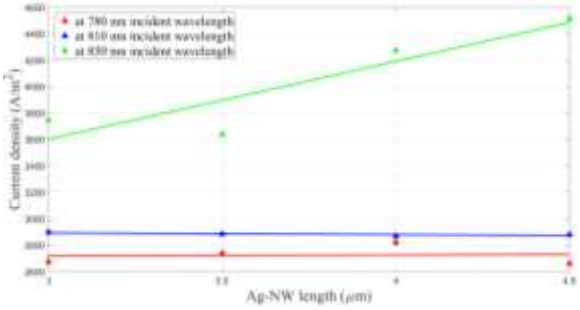

Fig.7: Calculated current density (colored triangles) in the photomixer active region as a function of Ag-NWs lengths. The colored lines represent the results fitted curves.

Table (1) Calculated SPPs Propagation length on the Ag-NW interface with GaAs substrate for the three excitation wavelengths.

Incident Wavelength (nm)	**780**	**810**	**850**
SPPs Propagation length (μm)	1.7	2.4	3.4

As it can be seen from the table and according to Eq. (5), L_{SPP} is directly proportional to the excitation wavelengths. By substituting the calculated values of L_{SPP} in Eq. (4), propagation losses are obtained for each value of L_{NW}. Fig. (8) shows the calculated propagation losses of SPP on the Ag-NW interface with GaAs as function of L_{NW} for the three excitation wavelengths. From the results, it can be seen that the propagation losses are decreased at longer L_{NW}.

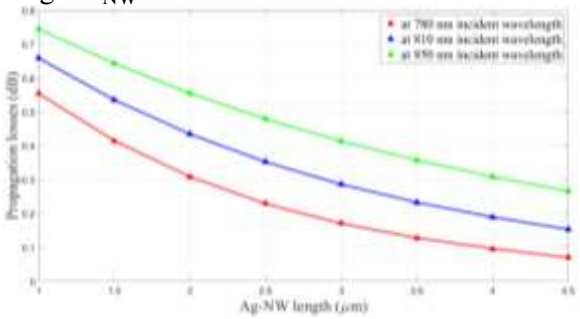

Fig.8: Calculated propagation losses of SPP (colored triangles) on the Ag-NW interface with GaAs as function of L_{NW} for three excitation wavelengths: 780, 810, and 850 nm. The colored lines represent the results fitted curves.

Due to this reduction in the propagation losses of SPP, the electric field in the active region shows an increment in its value with L_{NW}. Additionally, the longer wavelengths of light show the largest values of propagation losses, as it is seen in Fig. (8). Therefore, the simulation results exhibit remarkable change in the electric field with L_{NW} at the longer values of wavelengths.

The 780 and 850 nm excitation wavelengths exhibits higher plasmonic effect of Ag-NW, where the electric field is enhanced by the factor of two after adding the nanowires, as shown in Fig. (2). While the field shows a small change in its value at 810 nm wavelength. This change has grown when the Ag-NW number and length are increased. The maximum response of electric field to the change in the Ag-NW number and length is obtained at the two longer wavelengths (810 and 850 nm). This response becomes a small at 780 nm wavelength where the electric field is less affected by Ag-NW number and length, as shown is Fig.(2), and (5) respectively.

The increment of Ag-NWs length and number can contribute to increase the electric field in the active region by 1.5 times at 850 nm. According to Eq. (1), THz output power is quadratically proportional to incident intensity $P_{THz\,(\omega_{THz})} \propto I_o^2$. Therefore, it is proportional to the fourth power of the electric field. Since the electric field is increased by 1.5 times with increasing the nanowire parameters, it can be expected from Eq. (1) that P_{THz} is enhanced by a factor of five. Additionally, the optical to THz conversion efficiency is also improved by a factor of five according to Eq. (2).

Consequently, the length of 4.5 μm is the best L_{NW} value for THz photomixer emitter that uses two Ag-NWs or more as nanoelectrodes and has a surface area of 10 x 10 μm^2. Therefore, reducing L_{NW} in order to decrease Ag-NWs gap and subsequently, minimize the device capacitance leads to bring down the electric field in the active region especially at longer wavelength value.

4. Conclusions

Increasing Ag-NWs length to SPP propagation length ratio plays a significant role on field increment due to its effect on reducing the SPP propagation losses. The increment of Ag-NWs length and number in the Ag-NWs based photomixer can contribute to increase the electric field in the active region by 1.5 times at the longer excitation wavelength (850 nm). The length of 4.5 μm is the best L_{NW} value for THz photomixer emitter that uses two Ag-NWs or more as nanoelectrodes and has a surface area of 10 x 10 μm^2. As a result of the notable increment in the electric field, the THz output power and the conversion efficiency are expected to be enhanced by a factor of five.

References

[1] R. Safian, G. Ghazi, and N. Mohammadian, "Review of photomixing continuous-wave terahertz systems and current application trends in terahertz domain", Optical Engineering, **58**, 1–28 (2019).

[2] I. S. Gregory *et al.*, "Optimization of photomixers and antennas for continuous-wave terahertz emission", IEEE J. Quantum Electron., **41**, 717–728 (2005).

[3] S. Preu, G. H. Döhler, S. Malzer, L. J. Wang, and A. C. Gossard, "Tunable, continuous-wave Terahertz photomixer sources and applications", J. Appl. Phys., **109**, 061301 (2011).

[4] D. Saeedkia, R. R. Mansour, and S. Safavi-Naeini, "The interaction of laser and photoconductor in a continuous-wave terahertz photomixer", IEEE J. Quantum Electron., **41**, 1188–1196 (2005).
[5] D. Saeedkia, R. R. Mansour, and S. Safavi-Naeini, "Modeling and Analysis of High-Temperature Superconductor Terahertz Photomixers", IEEE Trans. Appl. Supercond., **15**, 3847–3855 (2005).
[6] E. R. Brown, "THz Generation by Photomixing in Ultrafast Photoconductors", International Journal of High Speed Electronics and Systems, **13**, 497-545 (2003).
[7] E. Pliński, "Terahertz photomixer", Bulletin of the Polish Academy of Sciences: Technical Sciences, **58**, 463-470 (2010).
[8] S. Lepeshov, A. Gorodetsky, A. Krasnok, E. Rafailov, and P. Belov, "Enhancement of terahertz photoconductive antenna operation by optical nanoantennas: Enhancement of terahertz photoconductive antenna operation by optical nanoantennas", Laser & Photonics Reviews, **11**, 1600199 (2017).
[9] A. D. J. F. Olvera, H. Lu, A. C. Gossard, and S. Preu, "Continuous-wave 1550 nm operated terahertz system using ErAs:In(Al)GaAs photo-conductors with 52 dB dynamic range at 1 THz", Opt. Express, **25**, 29492 (2017).
[10] D. J. Ironside, R. Salas, P.-Y. Chen, K. Q. Le, A. Alú, and S. R. Bank, "Enhancing THz generation in photomixers using a metamaterial approach", Opt. Express, **27**, 9481 (2019).
[11] C. W. Berry, N. Wang, M. R. Hashemi, M. Unlu, and M. Jarrahi, "Significant performance enhancement in photoconductive terahertz optoelectronics by incorporating plasmonic contact electrodes", Nature Communications, **4**, 1622 (2013).
[12] S.-H. Yang and M. Jarrahi, "Frequency-tunable continuous-wave terahertz sources based on GaAs plasmonic photomixers", Appl. Phys. Lett., **107**, 131111 (2015).
[13] R. Al-Mudhafar and H. A. Jawad, "Plasmonic hybrid terahertz photomixer of graphene nanoantenna and nanowires", IJECE, **12**, 2711 (2022).
[14] S. Al-Daffaie, O. Yilmazoglu, F. Kuppers, and H. L. Hartnagel, "1-D and 2-D Nanocontacts for Reliable and Efficient Terahertz Photomixers", IEEE Trans. THz Sci. Technol., **5**, 398–405 (2015).
[15] A. J. Jumaah, S. Al-Daffaie, O. Yilmazoglu, and T. Kusserow, "Continuous-wave terahertz emitter with hybrid nanoelectrodes based on graphene and nanowire", OSA Continuum, **3**, 1826 (2020).
[16] H. Arenhövel and D. Drechsel, Eds., "*Principles of Terahertz Science and Technology*", Berlin ; New York: Springer-Verlag, (1979).
[17] Z. Ruan, G. Veronis, K. L. Vodopyanov, M. M. Fejer, and S. Fan, "Enhancement of optics-to-THz conversion efficiency by metallic slot waveguides", Optics express, **17**, 13502-13515 (2009).
[18] A. W. Sanders, D. A. Routenberg, B. J. Wiley, Y. Xia, E. R. Dufresne, and M. A. Reed, "Observation of Plasmon Propagation, Redirection, and Fan-Out in Silver Nanowires", Nano Lett., **6**, 1822–1826, (2006).
[19] P. Venugopalan, Q. Zhang, X. Li, and M. Gu, "Polarization-sensitive characterization of the propagating plasmonic modes in silver nanowire waveguide on a glass substrate with a scanning near-field optical microscope", Opt. Express, **21**, 15247, (2013).
[20] Z. Fang, Y. Lu, L. Fan, C. Lin, and X. Zhu, "Surface Plasmon Polariton Enhancement in Silver Nanowire–Nanoantenna Structure", Plasmonics, **5**, 57–62, (2010).
[21] H. Ditlbacher *et al.*, "Silver Nanowires as Surface Plasmon Resonators", Phys. Rev. Lett., **95**, 257403, (2005).
[22] T. Laroche and C. Girard, "Near-field optical properties of single plasmonic nanowires", Appl. Phys. Lett., **89**, 233119, (2006).
[23] D. Buczyńska *et al.*, "Correlating Plasmon Polariton Propagation and Fluorescence Enhancement in Single Silver Nanowires", J. Phys. Chem. C, **124**, 15418–15424, (2020).
[24] M. Jablan, H. Buljan, and M. Soljačić, "Plasmonics in graphene at infrared frequencies", Phys. Rev. B, **80**, 245435, (2009).
[25] A. S. Kalmykov, R. V. Kirtaev, D. V. Negrov, P. N. Melentiev, and V. I. Balykin, "Surface plasmon wave propagation length measurement at a telecom wavelength", Laser Phys. Lett., **17**, 045901, (2020).

تأثيرعدد وحجم الأقطاب النانوية على أداة الدامج الضوئي لاشعة THz

ريام ضياء محمدرضا حسين علي جواد

معهد الليزر للدراسات العليا ، جامعة بغداد ، بغداد ، العراق

الخلاصة: بالرغم من السمات المميزة لباعث الموجة المستمرة (CW) تيراهيرتز (THz) باستخدام تقنية المزج الضوئي ، إلا أنه يعاني من طاقة خرج إشعاع منخفضة نسبيًا. لذلك ، كانت إحدى الطرق الفعالة لتحسين أداء باعث المزج الضوئي هي استخدام أقطاب نانوية داخل المنطقة الضوئية النشطة للجهاز. نظرًا للأحجام النانوية والتوصيل الكهربائي الجيد للأسلاك النانوية الفضية (Ag-NWs) ، تم استغلالها كأقطاب باعث THz. تعمل موجات البلازمونات السطحية (SPPs) المثارة على سطح الأسلاك النانوية على تعزيز إشارة الإستثارة الساقطة. لذلك ، فإن المزج الضوئي القائم على-Ag NW مقارنة بالآخر التقليدي يعرض بشكل ملحوظ إشارة خرج THz أعلى. في هذا العمل ، تم التحقيق في تأثير أبعاد Ag-NWs وعددها على المجال الضوئي الساقط من خلال استخدام برنامج Studio Simulation Technology (CST). اظهرت نتائج المحاكاة أن زيادة طول Ag-NWs إلى نسبة طول انتشار SPP تلعب دورًا مهمًا في زيادة المجال الساقط نظرًا لتأثيرها على تقليل خسائر انتشار SPP. يمكن أن تساهم الزيادة في عدد Ag-NWs وطولها في المزج الضوئي المستند إلى الأقطاب النانوية في زيادة المجال الكهربائي في المنطقة النشطة بمقدار 1.5 مرة عند الطول موجي الأطول (850 نانومتر). نتيجة لهذة الزيادة في المجال الكهربائي ، من المتوقع أن يتم تعزيز قدرة خرج THz وكفاءة التحويل بمعامل خمسة.